STRUCTURE OF THE EARTH'S MAGNETOPAUSE

Bengt U.O. Sonnerup*
+ Royal Institute of Technology
Stockholm, Sweden

and

Laurence J. Cahill, Jr.
Department of Physics
University of New Hampshire, Durham

*Present Address: Radiophysics Laboratory, Dartmouth College
Hanover, New Hampshire

+This research was partially supported by the National Aeronautics and Space Administration under Contract NASw-155 and Grant NsG-624

STRUCTURE OF THE EARTH'S MAGNETOPAUSE

Bengt U.O. Sonnerup*
Royal Institute of Technology
Stockholm, Sweden

and

Laurence J. Cahill, Jr.
Department of Physics
University of New Hampshire, Durham

ABSTRACT

14954

Five Explorer 12 magnetometer records are examined with the objective of deciding whether the terrestrial magnetic-field lines on the sunlit side of the magnetosphere reach into interplanetary space. It is shown how the data can be used to determine the vector normal to the magnetopause surface. The field component along this normal vector is computed. In three cases, all occurring during magnetic-storm main phases, normal-field component of 7-8 γ are found. In at least one of these cases this result cannot readily be explained by experimental errors. Of the two remaining cases, occurring during magnetically quiet conditions, one was inconclusive and the other showed an insignificantly small normal-field component. The measured normal vector is found to deviate substantially from theoretical predictions suggesting waves or local bumps in the magnetopause surface. In one of the storm cases a tongue of the interplanetary medium seems to have penetrated more than one earth radius into the magnetosphere.

Author

*Present Address: Radiophysics Laboratory, Dartmouth College
Hanover, New Hampshire

INTRODUCTION

The first extensive observations of the boundary of the geomagnetic field, the so-called magnetopause, on the sunlit side of the magnetosphere were made from the Explorer 12 satellite (Cahill and Amazeen, 1963). The transition from the terrestrial to the compressed interplanetary field was usually accompanied by an abrupt change of the field direction. This implies the existence of a current sheet at the boundary. Furthermore, it was found that the external field frequently had a direction roughly opposite to that of the geomagnetic field just inside the boundary. Such a situation is favorable for the occurrence of an open magnetosphere where the earth's polar field lines reach into interplanetary space (Fig. 1). This is the model discussed by Dungey (1961, 1963), and more recently by Petschek (1964). On the other hand, a closed magnetosphere is also possible in this case. Here the terrestrial field lines are entirely confined to the geomagnetic cavity as shown in Figure 2. In both cases the field reversal on the sunlit side of the magnetosphere can be accomplished by a thin current sheet. However, an important difference is that the magnetic-field component perpendicular to, and within, this thin current-layer should be very small for the closed magnetosphere whereas a substantial perpendicular component could occur in the open case. From the topological viewpoint a distinguishing feature is the existence of X-type magnetically neutral points in the current layer of the open model and of O-types in that of the close one; see Figures 1 and 2. Our discussion will be confined to these two magnetosphere models even though they are not the only conceivable ones.

In the present paper we examine in detail five selected Explorer 12 magnetometer records at the magnetopause with the objective of deciding whether the magnetosphere was closed or open.

A vector normal to the boundary surface is derived from the measurements and the magnetic-field component perpendicular to the surface is computed. Also, we estimate the location of the singular field line which runs along the boundary and connects the two X-type neutral points (A and B in Fig. 1) in the open magnetosphere. When the interplanetary and terrestrial fields are exactly antiparallel this line lies in the geomagnetic equatorial plane. For more general interplanetary-field directions the configuration has been described in detail by Dungey (1963). The two results are then checked for consistency; the perpendicular field component should be directed outward from the earth if the point of the boundary penetration is located below the singular field line and inward if the penetration point occurs above it. See Figure 1.

Finally, the measured normal vector is compared to a theoretical normal vector obtained by assuming that the magnetopause has the shape found by Mead and Beard (1964).

MEASUREMENTS

For a detailed description of the Explorer 12 magnetometer experiment and the orbit we refer to the paper by Cahill and Amazeen (1963). The measurements are presented in terms of the field magnitude (F) and the two angles λ and ψ which define the field direction relative to the spin axis of the satellite and the earth-sun line as shown in Figure 3. The direction of the spin axis, determined by analysis of solar aspect data, was -27.5° declination at 47° right ascension in celestial coordinates. If this direction is instead determined by comparison of the magnetic data to the terrestrial dipole field at 30000 km the magnitude of the declination is found to be about 10° less. This uncertainty does not affect the determination of the normal-field component but it should be kept in mind when measured fields and normal vectors are compared with theoretical ones. The direction determined from solar aspect data is used throughout this paper.

A compilation of the basic information concerning the five boundary crossings to be discussed here is given in Table 1. The colum labelled 'local time' gives the local time of the subsatellite point on earth at the boundary penetration. The behavior of the field vector at the boundary is shown in Figures 4 through 8. In these diagrams every complete measurement of the quantities (F), λ and ψ is recorded. The satellite makes approximately three complete measurements per second. The absence of data points indicates that no measurements are available becuase of magnetometer calibration or for other reasons.

Finally, in order to get an overall picture of the magnetic field at larger distances from the boundary, the less detailed survey diagrams, Figures 9 through 12, may be used.

In these graphs a single point represents an average of twenty consecutive individual measurements and between the points many measurements are available which have not been used in preparation of the plots.

TABLE I

Date (1961)	Inbound Outbound	Universal Time	Geocentric Dist. (km)	Geographic Longitude	Geographic Latitude	Geomag. Latitude	Local Time
09/03	i	16.48.50	67500	-71.4°	-3.5°	8.2°	12:03
09/30	o	18.49.55	66580	-157.2°	-18.7°	-17.9°	08:21
10/01	i_1	09.34.30	63740	12.8°	$.6^{\circ}$	2.3°	10:25
10/01	i_2	10.42 30	56670	$-.5^{\circ}$	3.2°	7.4°	10:41
10/29	i	01.59.35	61520	101.4°	4.0°	-7.6°	08.46

Because of the $\pm$ 12 γ uncertainty in the magnitude of the field components introduced by the digitization of the Explorer 12 data we have chosen only to consider boundary crossings which occurred at a high magnetic-field intensity. In this respect the cases reported here are not representative of the majority of the boundary crossings. Also, the boundaries were picked to have a rapid and well-defined field reversal whereas in many other cases the transition occurred more gradually and/or involved only moderate changes of the field direction. Rapid transitions are preferred to slow ones since the former case it is more reasonable to interpret the field mapping obtained by Explorer 12 as a true picture of a stationary or moving time-independent boundary structure.

Finally, it should be pointed out that the last three of the boundary crossings in Table 1 occurred during the main phase of magnetic storms. Also, on the inbound pass of October 1 several boundary penetrations occurred of which only the two first ones are reported here. It appears that on this occasion the boundary moved back and forth past the satellite. This may also have been the case on September 3 (see Fig. 9).

INTERNAL AND EXTERNAL FIELDS

The field directions on either side of the boundary are determined by forming the average of the angles α and ψ for a number of individual measurements. The points involved in this process are indicated in Figures 4-8. It may be noted that the points corresponding to the lowest values of the field intensity (F) have been excluded since the determination of the angles becomes very inaccurate at low fields. These points appear in parantheses in the diagrams. The resulting field vectors are expressed in a right-hand cartesian coordinate system ($\underline{t}_1$, $\underline{t}_2$, $\underline{t}_3$) defined as follows

$$\underline{t}_1 \equiv \underline{t}_2 \times \underline{t}_3 \tag{1}$$

$$\underline{t}_2 \equiv (\underline{\omega} \times \underline{d}) / |\underline{\omega} \times \underline{d}| \tag{2}$$

$$\underline{t}_3 \equiv \underline{d} \tag{3}$$

Here $\hat{d}$ is a unit vector due north along the earth's magnetic dipole axis and $\hat{\omega}$ is the unit vector along the undisturbed solar-wind velocity. The solar wind is taken to be radial from the sun but an abberation angle of 5° caused by the orbital motion of the earth is taken into account in the computation of $\underline{\omega}$. In Table II the magnitudes and direction cosines relative to these axes are given for the field vectors $\underline{F}_i$ and $\underline{F}_o$ inside and outside the magnetopause, respectively.

TABLE II

Date (1961)	$\lvert F_i \rvert$ γ	$\frac{\underline{F}_i \cdot \underline{\xi}_1}{\lvert F_i \rvert}$	$\frac{\underline{F}_i \cdot \underline{\xi}_2}{\lvert F_i \rvert}$	$\frac{\underline{F}_i \cdot \underline{\xi}_3}{\lvert F_i \rvert}$	$\lvert F_o \rvert$ γ	$\frac{\underline{F}_o \cdot \underline{\xi}_1}{\lvert F_o \rvert}$	$\frac{\underline{F}_o \cdot \underline{\xi}_2}{\lvert F_o \rvert}$	$\frac{\underline{F}_o \cdot \underline{\xi}_3}{\lvert F_o \rvert}$
09/03i	50	-.248	-.208	.946	47	-.165	.728	-.666
09/30o	54	.171	-.712	.681	49	-.247	.444	-.862
10/01i_1	57	-.294	-.939	.182	70	.001	.663	-.748
10/01i_2	82	.618	-.016	.786	95	.506	.493	-.708
10/29i	70	.007	-.555	.832	72	.194	.876	-.442

Since all boundary-penetrations occur rather near the geomagnetic equatorial plane (Table 1) one would, for simple permanently closed magnetosphere models (Mead, 1964) expect the internal-field vector to lie mainly along the $\underline{\xi}_3$ axis. It is clear by inspection of column 5 in Table II that the internal field frequently deviates strongly from such models. In particular this is the case for the first inbound crossing on October 1, (10/01/i_1). Note also that the external field tends to oppose the terrestrial field in the cases considered here.

NORMAL-FIELD COMPONENT

If the current layer is thin the normal-field component should be continuous across the layer. In other words, the relations

$$\underline{F}_i \cdot \underline{n} = \underline{F}_o \cdot \underline{n} = \underline{F} \cdot \underline{n} \qquad (4)$$

should hold. Here $\underline{n}$ denotes the vector normal to the current layer, $\underline{F}_i$ and $\underline{F}_o$ are the average fields just inside and outside of the layer and $\underline{F}$ is the field vector at an arbitrary point in the current-layer interior. These relations require $\underline{n}$ to be proportional to the vector

$$\underline{N} = \underline{F}_i \times \underline{F}_o - (\underline{F}_i - \underline{F}_o) \times \underline{F} \tag{5}$$

It is easily seen that $\underline{F}_i$, $\underline{F}_o$ and $\underline{F}$ have the common component $\underline{F} \cdot (\underline{F}_i \times \underline{F}_o)/|\underline{N}|$ along this vector. Note also that the vector $(\underline{F}_i - \underline{F}_o)$ is a tangent to the surface. For each individual measurement of F in the current-layer interior a corresponding $\underline{N}$ -vector can be formed and our approximation for the true normal vector is taken to be the normalized average of all the $\underline{N}$ -vectors thus computed. In other words, we have

$$\underline{n} = \pm \frac{(\underline{F}_i \times \underline{F}_o) - (\underline{F}_i - \underline{F}_o) \times \overline{\underline{F}}}{|(\underline{F}_i \times \underline{F}_o) - (\underline{F}_i - \underline{F}_o) \times \overline{\underline{F}}|} \tag{6}$$

where $\overline{F}$ denotes the average of all the field vectors measured in the current-layer interior. Also, the ambiguous sign in the formula is chosen so that $\underline{n}$ is directed outward. This method of determining the normal vector is useful except in the special case when

$$\underline{F}_i \times \underline{F}_o = (\underline{F}_i - \underline{F}_o) \times \overline{\underline{F}} \tag{7}$$

Equation (7) implies that $\underline{F}_i$, $\underline{F}_o$ and $\overline{\underline{F}}$ all have the same vector components in the plane perpendicular to the vector $(\underline{F}_i - \underline{F}_o)$. This in turn means that any vector perpendicular to $(\underline{F}_i - \underline{F}_o)$ is an adequate normal vector. Hence, it is impossible to determine the sign and magnitude of the field component along $\underline{n}$. In practice this case should arise occasionally. For example, it may be shown that Eq. (7) is satisfied if the current vectors in the current-layer interior are purely unidirectional which is possible if the magnetosphere is closed. It turns out that the first of the cases considered here (09/03/i) very nearly satisfies Eq. (7). Therefore, the normal vector is indeterminate for that crossing. In all the other cases Eq. (5) could be used to compute the normal vector. This implies that the current direction must vary with position in the interior of the layer. The resulting field components along $\underline{n}$ are given in the second column of Table III.

TABLE III

Date (1961)	$\bar{\underline{F}} \cdot \underline{n}$ (γ)	$\bar{\underline{F}} \cdot \underline{q}$ (γ)	σ (γ)	$\sigma / \sqrt{m}$ (γ)
09/03/i	Indeterminate	-.5	14.9	1.9
09/30/o	1.4	.8	20.0	3.2
10/01/i_1	-7.9	8.4	12.4	1.6
10/01/i_2	-7.3	2.7	16.0	2.1
10/29/i	7.8	-3.4	15.7	2.1

The normal-field components thus computed are significant only if the vector $\bar{\underline{F}}$ has a significant component perpendicular to the plane containing the two field vectors $\underline{F}_i$ and $\underline{F}_o$. Hence, the product $\underline{q} \cdot \underline{F}$ where

$$q = \pm (\underline{F}_i \times \underline{F}_o) / |\underline{F}_i \times \underline{F}_o| \tag{8}$$

is also given in Table III along with the standard deviation σ of the individual products $\underline{q} \cdot \underline{F}$ from the average. The ambiguous sign in Eq. (8) is chosen so that $\underline{q}$ is directed outward. The last column in Table III contains the quantity $\sigma/\sqrt{m}$. m being the number of individual measurements used in the formation of the average. This quantity represents the standard deviation of the computed average value from the true average, provided that all the individual field vectors in the current-layer interior have the same average component along $\underline{q}$ and the same standard deviation.

We conclude that with a high degree of probability a significant magnetic-field component perpendicular to the current-layer surface was present at the first inbound corssing on October 1, ($10/01/i_1$). Thus the magnetosphere was in all probability open on this occasion. Keeping in mind that there may also be some error in the vector $\underline{q}$ it appears somewhat less certain that the normal-field components for the cases ($10/01/i_2$ and (10/29/i) are significant. Finally, the normal-field component is clearly insignificant for the case (09/30/o) which occurred a few hours before the onset of the October 1 magnetic storm. Thus the magnetosphere may have been closed on that occasion but this is by no means certain. Other explanations are also possible.

At this point we also note that the large σ-values suggest that there must be appreciable local fluctuations in the field directions in the current-layer interior.

We may estimate the location of the boundary penetration point relative to the singular field line which runs along the boundary surface connecting the two X-type neutral points A and B in Figure 1. We call this the X line. It is along this line the cutting of frozen-in field lines is supposed to occur. This reconnection process which is necessary for the existence of the open magnetosphere has recently been discussed in detail by Petschek (1964). One of the X-type neutral points should occur at the forward stagnation point which, relative to the earth's center, is located in the direction of the negative solar-wind vector, $-\underline{\omega}$. If the boundary-penetration point lies near the stagnation point it is reasonable to assume the X line to run along the intersection between the magnetopause surface and a plane through the stagnation point which is parallel to the two vectors $\underline{I}$ and $\underline{w}$. $\underline{I}$ being the net-current vector at the boundary-penetration point. The vector $\underline{I}$ is parallel to $(F_i - F_o) \times n$. Hence, the boundary-penetration point is located above the X line if the product

$$P = \left[(\underline{F_i} - \underline{F_o}) \times \underline{n}\right] \cdot (\underline{b} \times \underline{\omega}) \qquad (9)$$

is negative and below it is P is positive. Here $\underline{b}$ is the unit vector in the direction from the earth's center to the boundary-penetration point. Also, the normal component, $\bar{F} \cdot \underline{n}$, of the field vector should be negative if the penetration point lies above the X line and positive if it lies below this line. In other words, P and $\underline{\bar{F}} \cdot \underline{n}$ should have the same sign. The result of this investigation is summarized in Table IV.

TABLE IV

Date (1961)	Sign of ρ	Sign of $\underline{F} \cdot \underline{n}$
$10/01/i_1$	-	-
$10/01/i_2$	-	-
10/29/i	-	+

We see that the signs are consistent for the two passages on October 1 and inconsistent for the case (10/29/i). However, this last boundary crossing occurred on the side of the magnetosphere far from the stagnation point. Our estimate of the location of the X line is probably very uncertain in this case.

THEORETICAL NORMAL VECTOR

We may also compare the measured normal vector, $\underline{n}$, with a theoretical normal vector, $\underline{n}_t$, obtained from Mead's and Beard's (1964) calculations for the case of a nonmagnetic interplanetary plasma. The simple formula

$$r/r_0 = 1.36 - 0.36 \cos \varphi_m \tag{10}$$

describes the sunlit side of their magnetosphere surface with an accuracy of $\pm$ 5% within geomagnetic latitudes, θ_m, of $\pm$ 45° (Mead, private communication). Here φ_m denotes the geomagnetic longitude and r_0 is the radius of the magnetosphere at the vertex point. Also, the formula applies only when the solar-wind vector, $\underline{\omega}$, lies in the geomagnetic equatorial plane. We use the same surface shpae also when $\underline{\omega}$ forms an angle λ with this plane.

However, the vertex point, located at the geocentric distance r_o, is placed at $\theta_m = \lambda/3$ in the plane containing the dipole asix, $\underline{d}$, and the solar-wind vector. This choice is arbitrary but reasonable. Furthermore, the axis of symmetry of Mead's surface is placed in the same plane but at an angle of $\lambda/2$ relative to the geomagnetic equatorial plane. It may be shown that for small λ values this gives the same slope of the magnetosphere surface at $\theta_m = \lambda/3$ as that of the boundary found by Spreiter and Briggs (1962), in the plane containing $\underline{d}$ and $\underline{\omega}$. The theoretical normal vector, thus determined, is compared with $\underline{n}$ and $\underline{q}$ in Table V. Also given is the angle λ. Note that q would be the normal vector if the magnetosphere were closed.

TABLE V

Date (1961)	$\underline{n}_t \cdot \underline{z}_1$ $\underline{n} \cdot \underline{z}_1$ $\underline{q} \cdot \underline{z}_1$	$\underline{n}_t \cdot \underline{z}_2$ $\underline{n} \cdot \underline{z}_2$ $\underline{q} \cdot \underline{z}_2$	$\underline{n}_t \cdot \underline{z}_3$ $\underline{n} \cdot \underline{z}_3$ $\underline{q} \cdot \underline{z}_3$	λ°
09/01/i	.978	.065	.196	
	---	---	---	20.7
	.818	-.478	-.320	
09/30/o	.825	-.500	-.264	
	.898	-.198	-.394	8.2
	.950	-.066	-.307	
10/01/i_1	.978	-.205	.022	
	.987	-.151	.057	-3.9
	.907	-.334	-.258	
10/01/i_2	.980	-.156	.121	
	.259	-.906	-.335	-.6
	.389	-.863	-.323	
10/29/i	.822	-.532	-.206	
	.995	-.051	.091	
	.925	-.314	-.217	-21.1

The agreement between $\underline{n}_t$ and either of $\underline{n}$ and $\underline{q}$ is in general rather poor. In particular this is the case for the crossing $(10/01/i_2)$. Regardless of whether the magnetosphere was open or closed on this occasion we must conclude that the magnetopause surface deviated strongly from the theoretical shape. There must have been large waves or bumps in the surface. As pointed out previously the boundary crossing $(10/01/i_2)$ was peculiar in that Explorer 12 was inside the magnetosphere and on its way towards the earth before the crossing. Apparently the magnetopause was then set in motion; it moved more than one earth radius and passed the satellite. Our computations of the vector normal to the magnetopause surface indicate that the inward motion of this surface may not have been caused by a uniform compression of the entire cavity. Rather it appears likely that a tongue of interplanetary plasma penetrated deep into the magnetosphere on this occasion. We emphasize that this particular event occurred during the main phase of a magnetic storm.

Another point worth mentioning is that no systematic improvement of the agreement between $\underline{n}_t$ and $\underline{n}$ or $\underline{n}_t$ and $\underline{q}$ would result by taking account of the possible effects of the spiral-shaped interplanetary field on the theoretical orientation of the geomagnetic cavity, (Walters, 1964). As a consequence of this we have not included these considerations in the computation of $\underline{n}_t$ or of the location of the stagnation point.

DISCUSSION

We have found some evidence of magnetic-field components perpendicular to the magnetopause surface during the main phase of the October 1, 1961, magnetic storm. On the other hand, the boundary crossing immediately before the sudden commencement of that storm revealed no significant such component. Thus, it appears likely that the magnetosphere was open during the storm main phase and it may have been closed immediately before the storm. Such a result would agree with the suggestion, (Sonnerup, 1964), that the onset of the main phase is caused by a change of the magnetospheric topology. However, other interpretations are probably also possible.

A more convincing proof of the existence of X-type neutral points would be provided by two consecutive boundary crossings occuring on opposite sides of the so-called X line, i.e. the field line joining the two neutral points. These two crossings should give normal-field components of opposite sign. Such cases may be contained in the Explorer 12 data but so far none have been found. In principle the O-type neutral points could be detected in the same way provided that the current layer is sufficiently thick to permit of measurable normal-field components in the current-layer interior. This condition is not fulfilled in the cases studied here.

The apparent current-layer thickness is of the order of 25 km for the boundaries studied here. The actual thickness could be larger is the boundary was moving past the satellite. If the measured deviations of the normal vector from the theoretical normal vector are caused by waves on the magnetopause surface it is reasonable to expect such motion. Also, in some cases, such as the inbound pass on October 1, 1961, there is direct evidence of boundary motion.

Petschek (1964) has interpreted the field-reversing current layer of the open magnetosphere as a standing Alfvén wave, a so-called rotational discontinuity, (Landau and Lifshitz, 1960). In a stationary state the field intensity must be the same on both sides of such a wave front as well as in its interior. The difference between $(\underline{F}_i)$ and $(\underline{F}_o)$ observed on October 1 (see Table II) could mean that the current layer was in a state of acceleration. Another point worth mentioning is the marked depression of the field intensity in the current-layer interior on September 30. This suggests that the layer did not have the character of a rotational discontinuity on that occasion.

According to Petscheck's theory the rate at which the frozen-in interplanetary field lines reconnect at the X line of the open magnetosphere is equal to the Alfvén speed based on the normal-field component at the current layer. Our results indicate that this speed is about 10% of the Alfvén speed based on the total field just outside the magnetopause. This result agrees with Petschek's predictions.

REFERENCES

Cahill, L. J. and P. G. Amazeen, The boundary of the geomagnetic field, *J. Geophys. Res.*, *68*, 1835-1843, 1963.

Dungey, J. W., Interplanetary magnetic field and the auroral zones, *Phys. Rev. Letters*, *6*, 47-48, 1961.

Dungey, J. W., the structure of the exosphere or adventures in velocity space; *In geophysics, the earth's environment*, Les Houches 1962, pp 525-537, Gordon and Breach, Science Publishers, 1963.

Landau, L. D. and E. M. Lifshitz, *Electrodynamics of continuous media*, Pergamon Press, 1960.

Mead, G. D., Deformation of the geomagnetic field by the solar wind, *J. Geophys. Res.* *69*, 1181-1195, 1964.

Mead, G. D. and D. B. Beard, Shape of the geomagnetic field solar wind boundary, *J. Geophys. Res.*, *69*, 1169-1179, 1964.

Petschek, H. E., Papers presented at the Solar-Wind Conference at California Institute of Technology, Pasadena, April, 1964. See also two Avco-Everett Research Laboratory papers: AMP 123, October 1963, H. E. Petschek, Magnetic field annihilation and Research Report 170, December 1963, R. H. Levy, H. E. Petschek and G. L. Siscoe, Aerodynamic aspects of the magnetospheric flow.

Sonnerup, B. U. O., On the occurrence of topological changes of the magnetosphere, Paper presented at the Solar-Wind Conference at California Institute of Technology, Pasadena, April 1964.

Spreiter, J. R. and B. R. Briggs, Theoretical determination of the form of the boundary of the solar corpuscular stream produced by interaction with the magnetic dipole field of the earth, *J. Geophys. Res.*, *67*, 37-51, 1962.

Walters, G. K., Effect of oblique interplanetary magnetic field on shape and behavior of the magnetosphere, *J. Geophys. Res.*, *69*, 1769-1783, 1964.

FIGURE CAPTIONS

Fig. 1 Magnetic-field line configuration of the open magnetosphere. The two X-type neutral points A and B are joined by the X-line along which the field reconnection occurs. When the interplanetary field is antiparallel to the equatorial dipole field the X-line lies in the geomagnetic equatorial plane. The dashed line indicates the location of the magnetopause.

Fig. 2 Magnetic-field line configuration of the closed magnetosphere when the external field is antiparallel to the equatorial dipole field.

Fig. 3 Vector diagram defining the angles α and ψ. The angle α lies between the magnetic-field vector F_m and the spin axis. The angle ψ lies between the plane containing the magnetic-field vector and the spin axis and the plane containing the sun direction and the spin axis.

Fig. 4 Complete magnetometer record for the inbound magnetopause penetration of September 3, 1961.

Fig. 5 Complete magnetometer record for the outbound magnetopause penetration on September 30, 1961.

Fig. 6 Complete magnetometer record for the first inbound magnetopause penetration on October 1, 1961.

Fig. 7 Complete magnetometer record for the second inbound magnetopause penetration on October 1, 1961.

Fig. 8 Complete magnetometer record for the inbound magnetopause penetration on October 29, 1961.

Fig. 9 Survey record of September 3, 1961, inbound pass. The boundary-penetration point analysed in the paper is indicated by an arrow.

Fig. 10 Survey record of September 30, 1961, outbound pass. The boundary-penetration point is indicated by an arrow.

Fig. 11 Survey record of October 1, 1961, inbound pass. The boundary-penetration points analysed in the paper are indicated by arrows.

Fig. 12 Survey record of October 29, 1961, inbound pass. The boundary-penetration point is indicated by an arrow.

FIG. 1

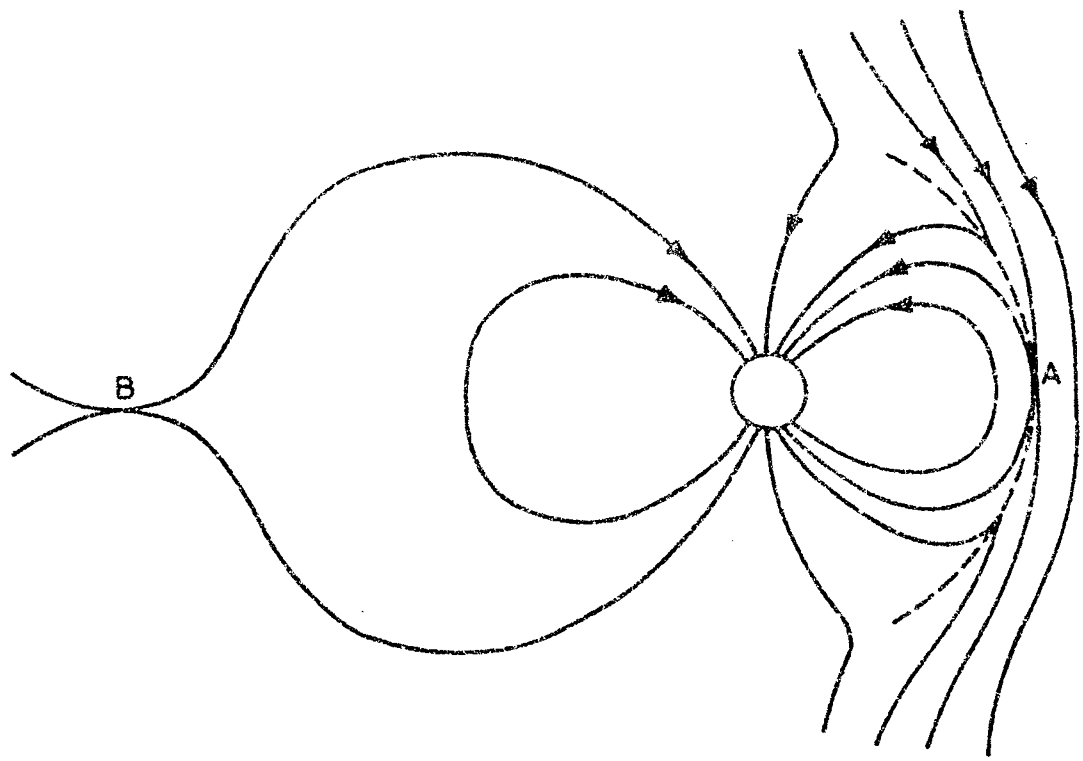

Fig. 1

FIG. 2

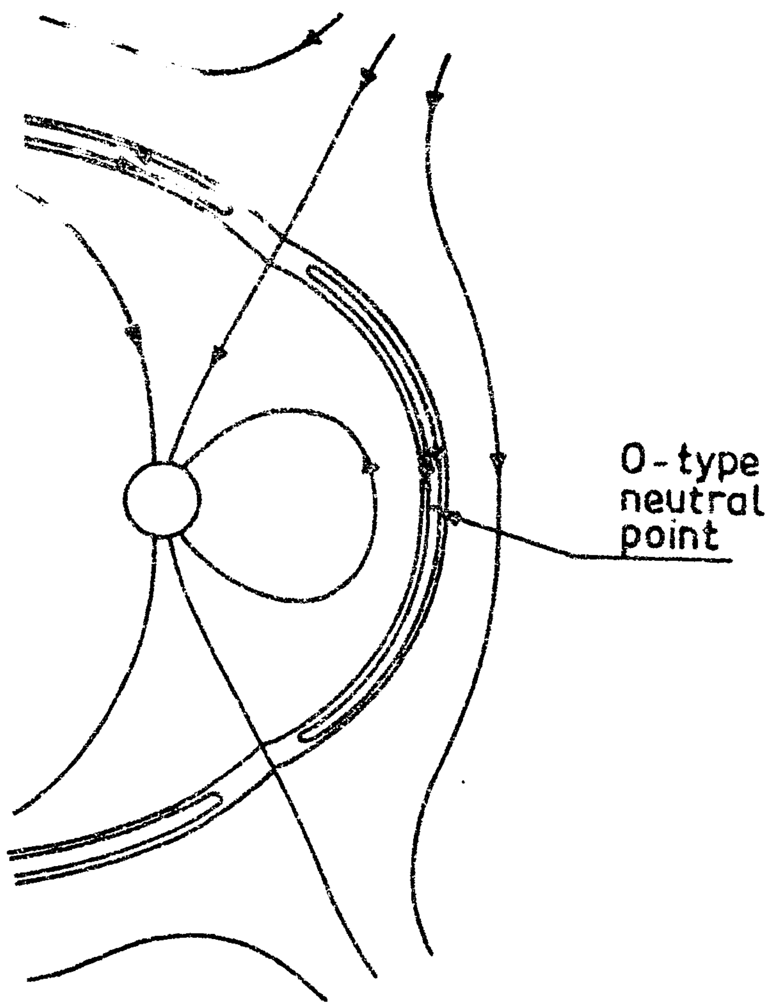

Fig. 2

Fɪɢ. 3

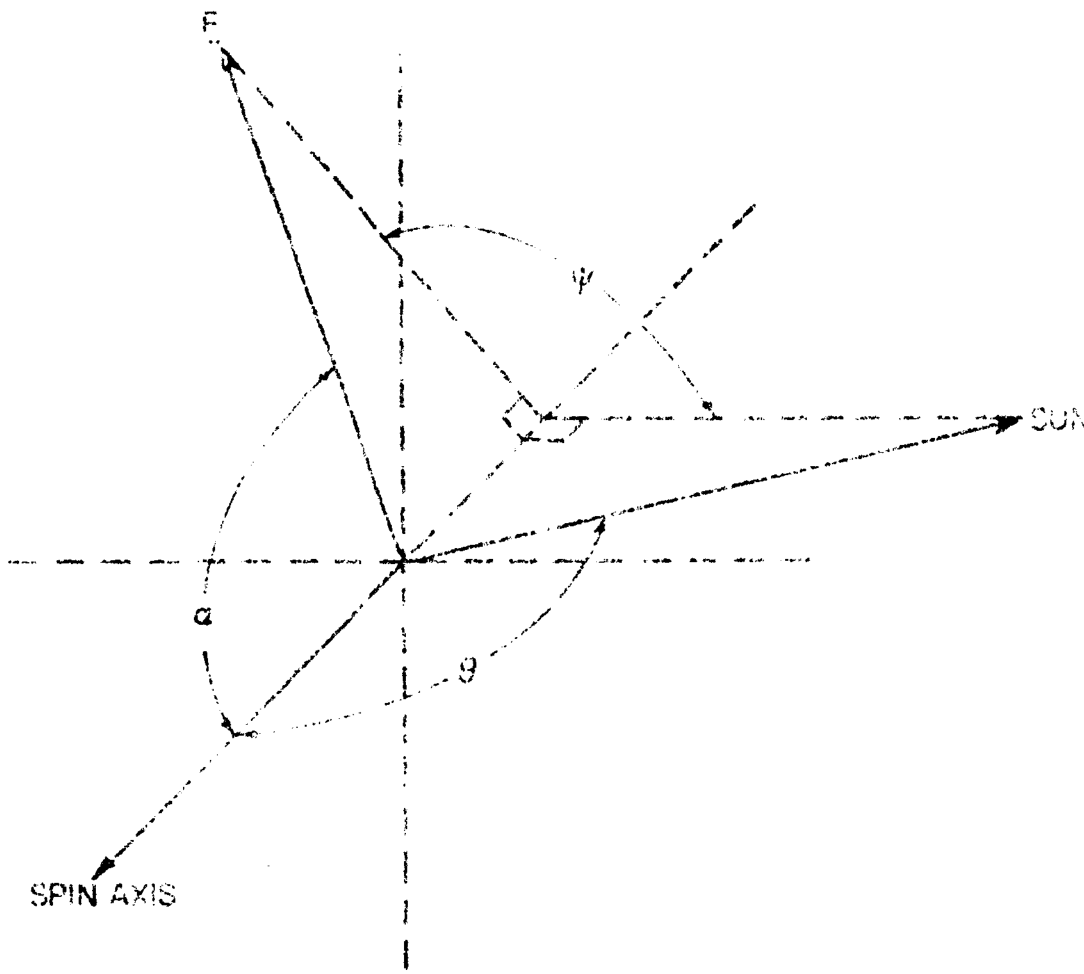

DIRECTION OF THE MAGNETIC FIELD IN RELATION TO THE SUN-SPIN PLANE.

FIG. 4

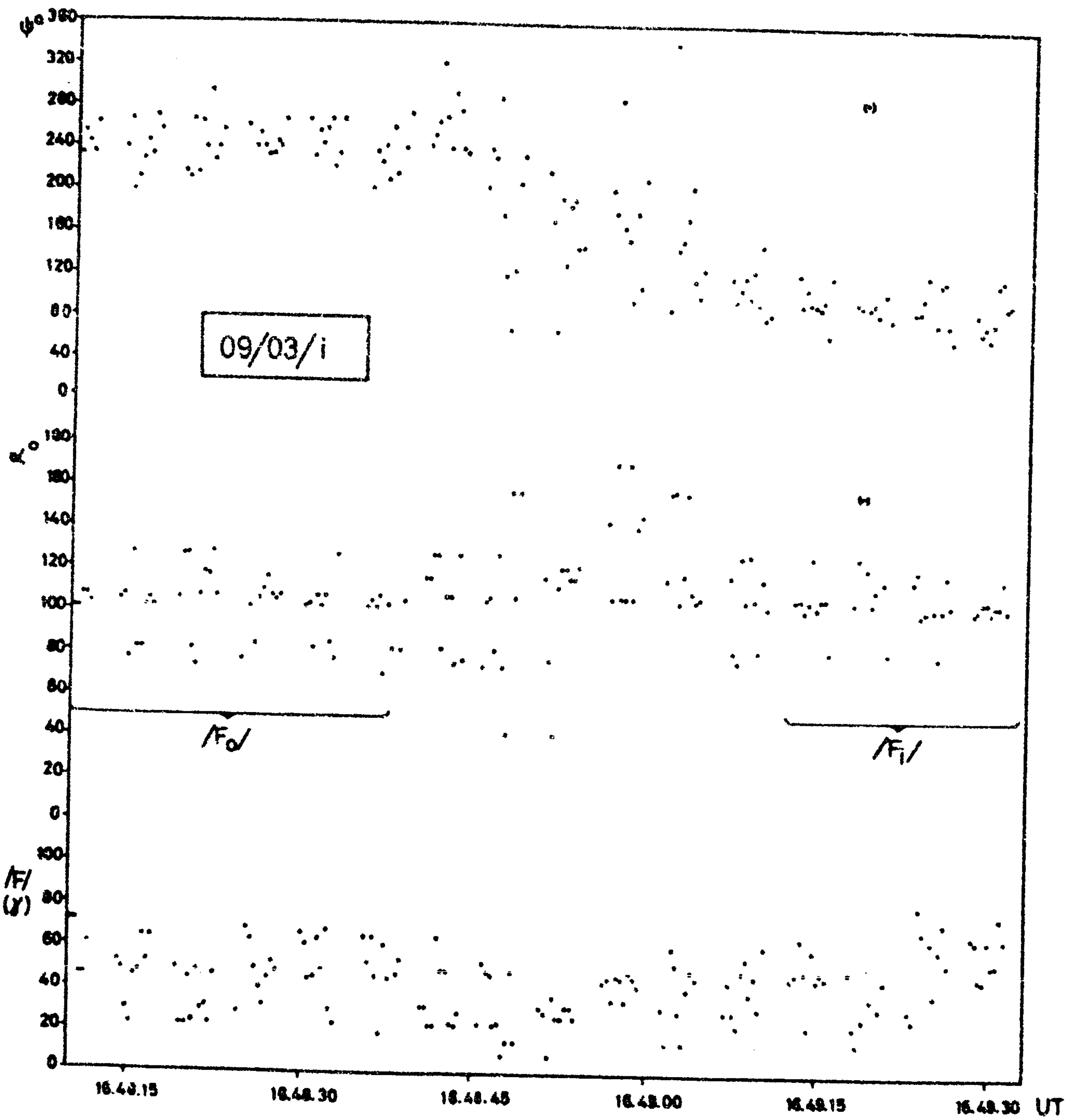

09/03/i
ψ°
α°
/F/ (γ)
/F₀/
/F₁/
16.48.15
16.48.30
16.48.45
16.49.00
16.49.15
16.49.30
UT

FIG. 5

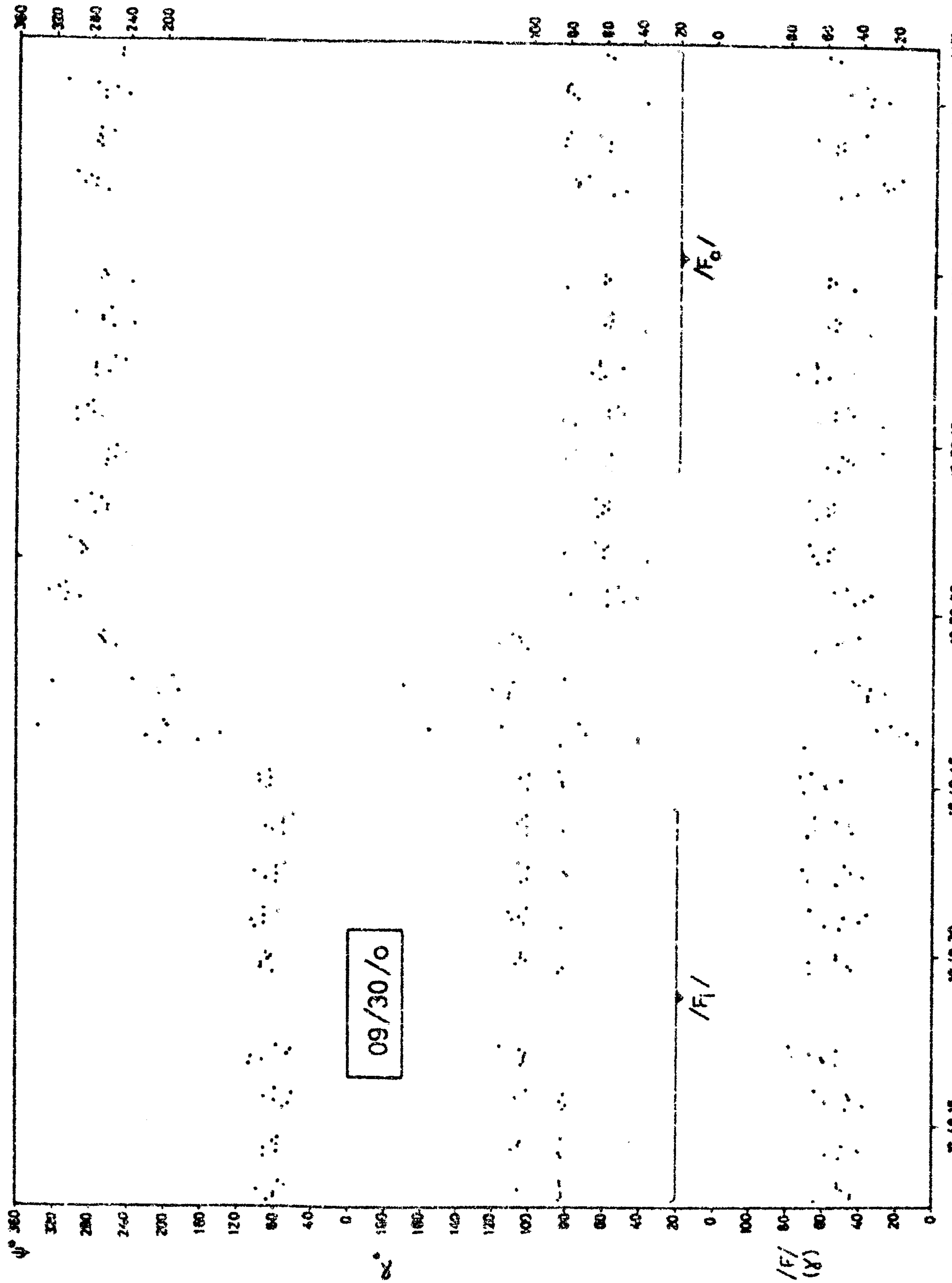

09/30/o
/F_o/
/F_i/
UT
18.49.15
18.49.30
18.49.45
18.50.00
18.50.15
18.50.30
18.50.45
ψ°
χ°
/F/ (γ)

Fig. 6

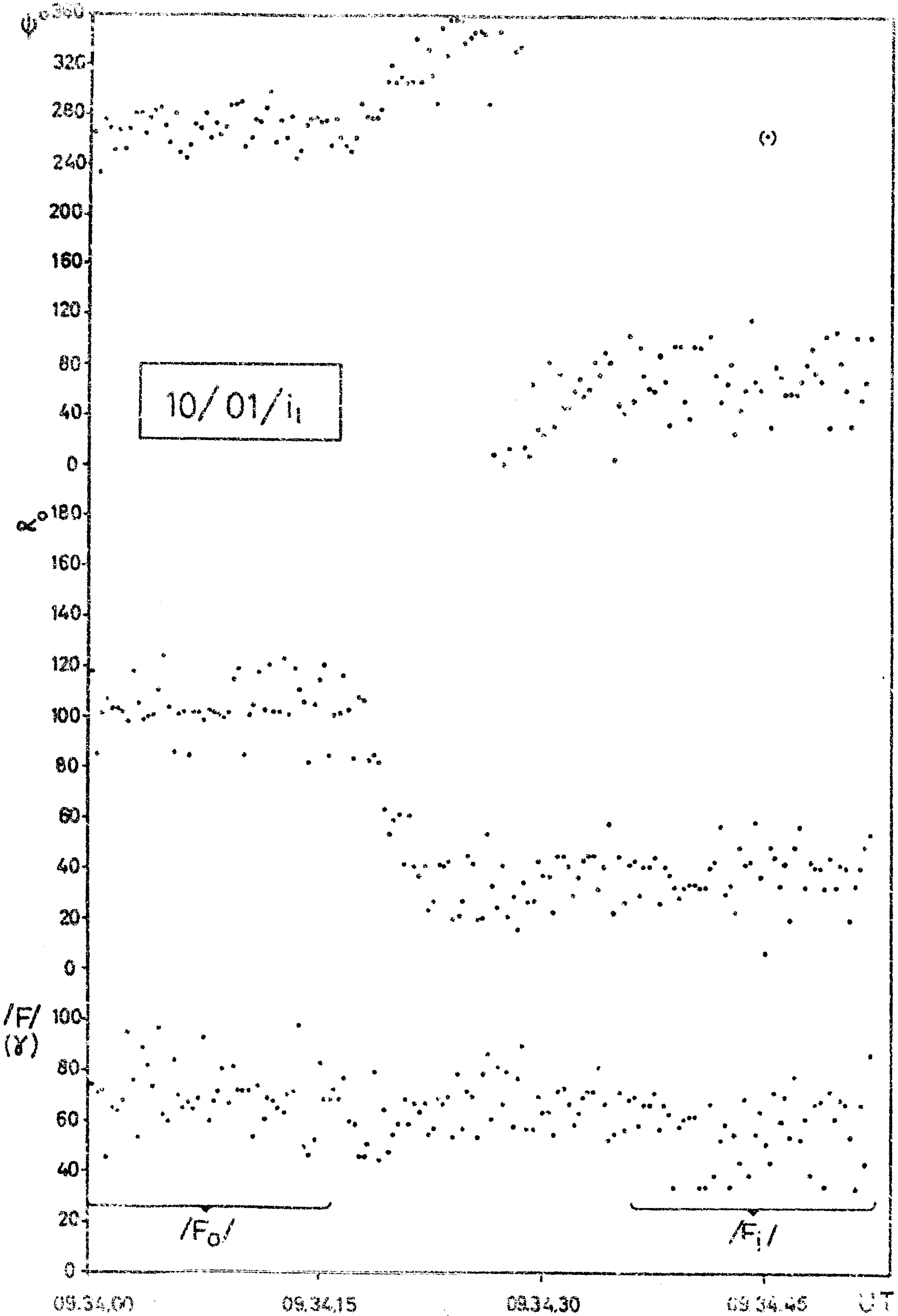

ψ° 360
320
280
240
200
160
120
80
40
0
α° 180
160
140
120
100
80
60
40
20
0
/F/ (γ) 100
80
60
40
20
0
10/01/i₁
/F₀/
/Fᵢ/
09.34.00
09.34.15
09.34.30
09.34.45
UT

FIG. 7

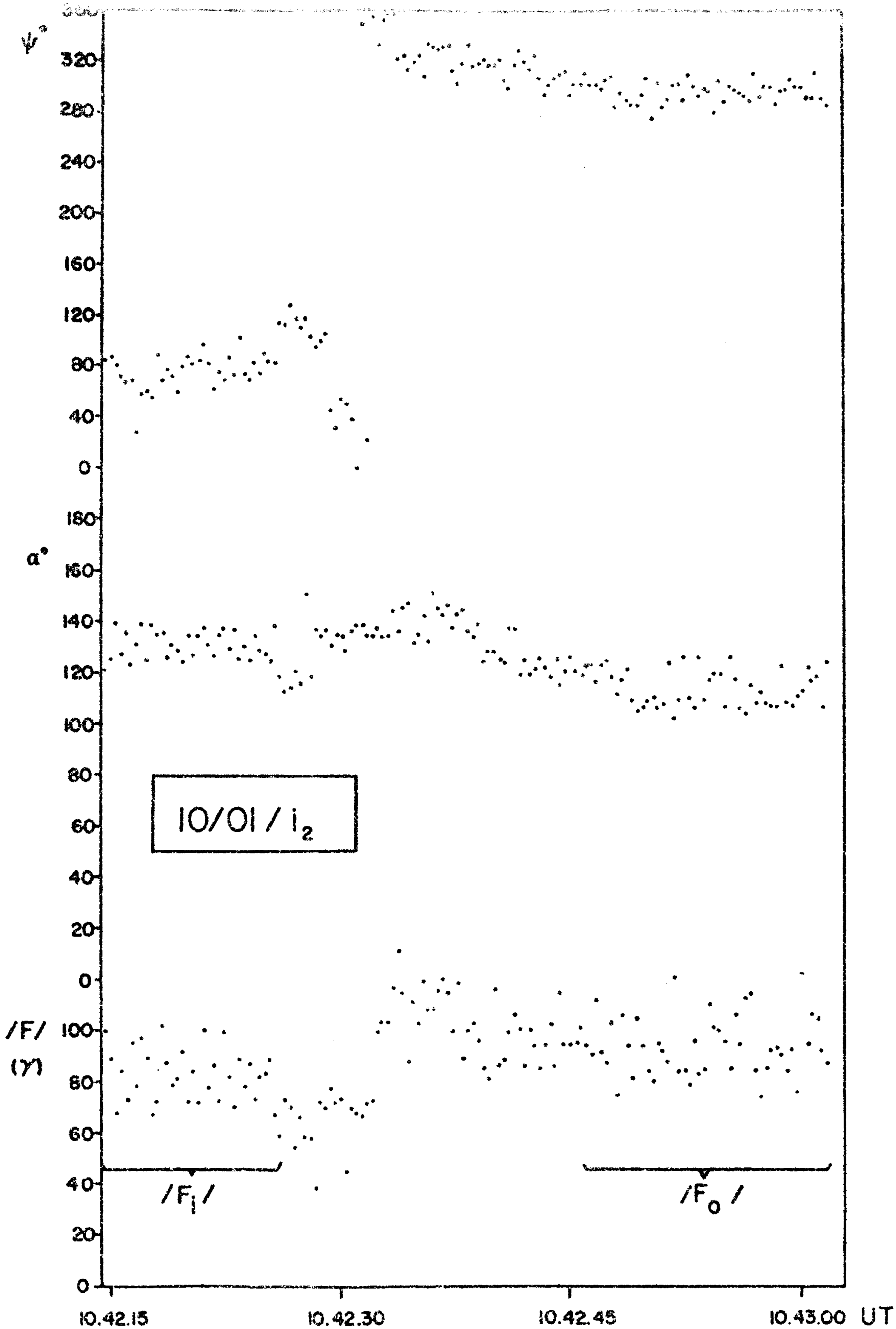

ψ°
320
280
240
200
160
120
80
40
0
180
α°
160
140
120
100
80
60
40
20
0
/F/
(γ)
100
80
60
40
20
0
10/01 / i_2
$/F_i/$
$/F_0/$
10.42.15
10.42.30
10.42.45
10.43.00
UT

FIG. 8

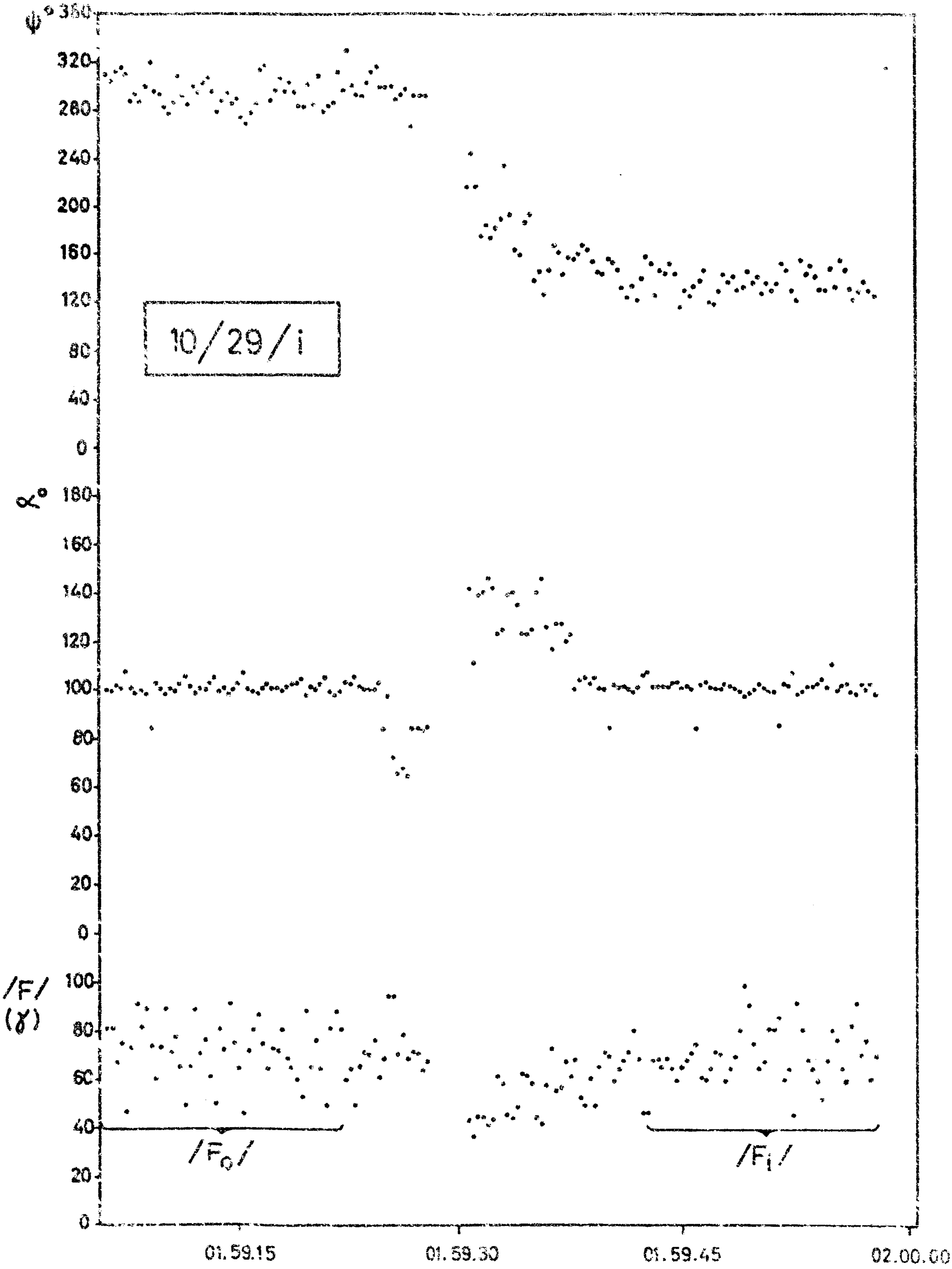

ψ°
360
320
280
240
200
160
120
80
40
0
α°
180
160
140
120
100
80
60
40
20
0
/F/
(γ)
100
80
60
40
20
0
10/29/i
/F₀/
/F₁/
01.59.15
01.59.30
01.59.45
02.00.00

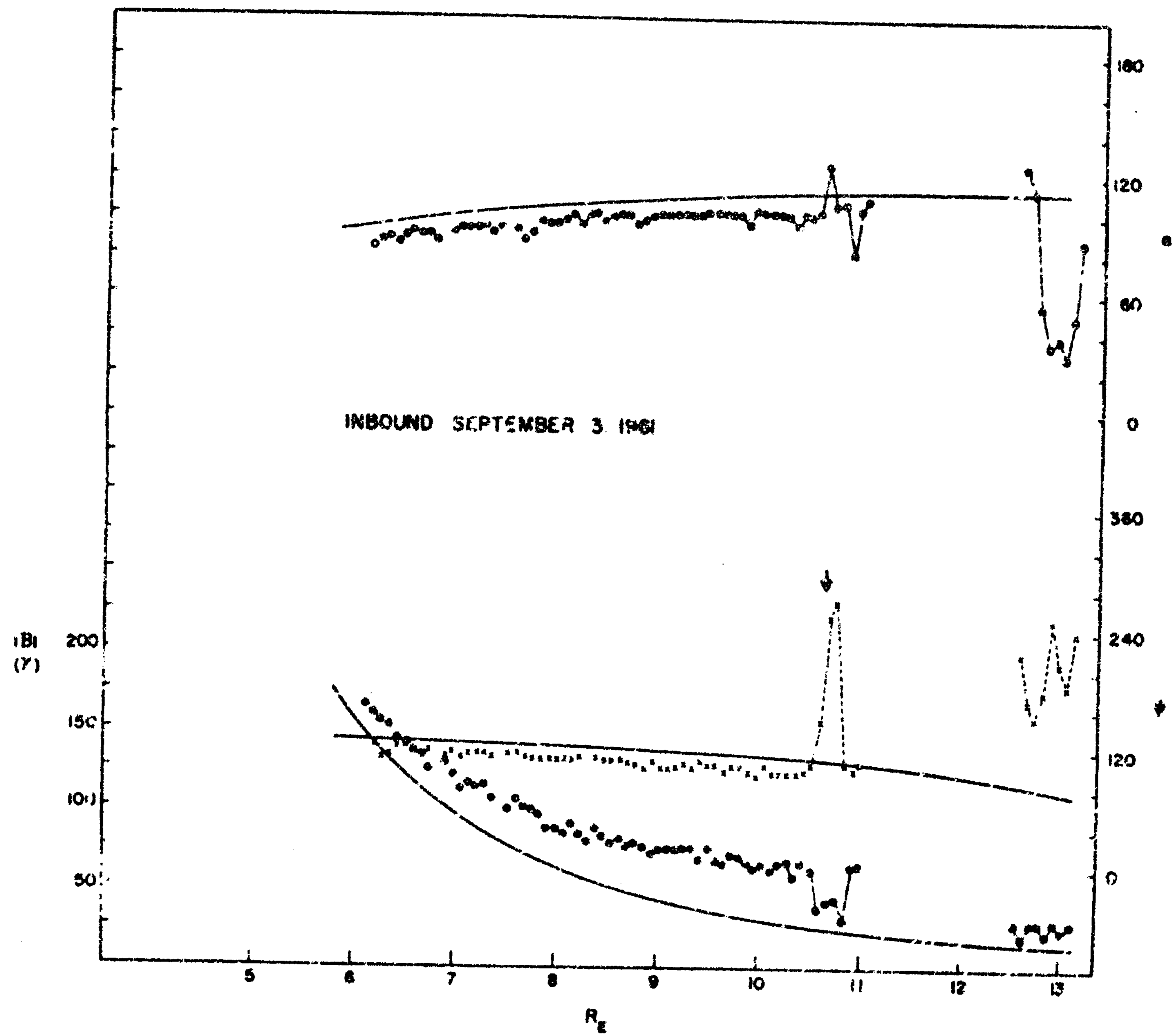
INBOUND SEPTEMBER 3 1961
|B| (γ)
200
150
100
50
5
6
7
8
9
10
11
12
13
R_E
180
120
60
0
θ
360
240
120
0
φ

FIG. 9

FIG. 10

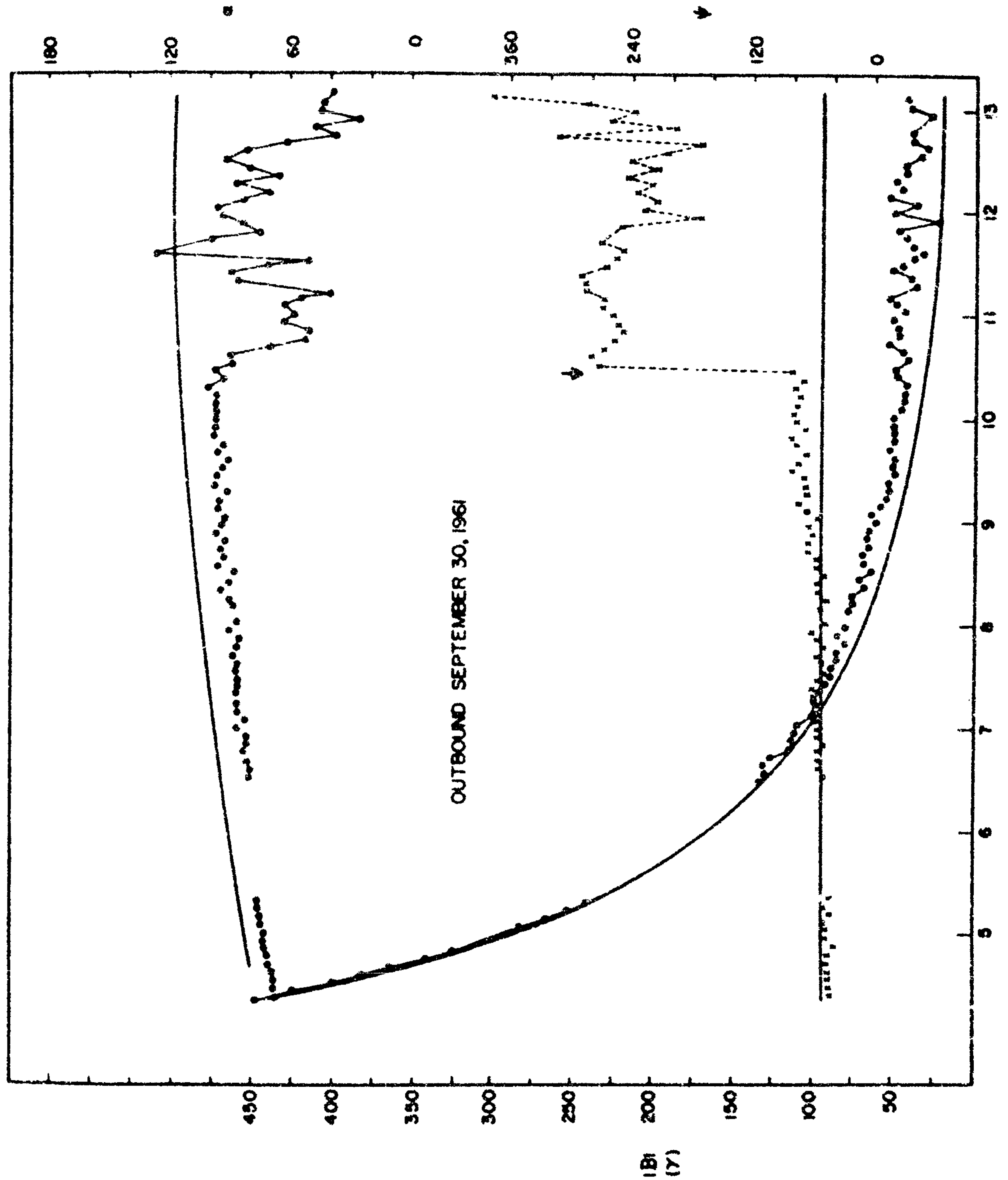

OUTBOUND SEPTEMBER 30, 1961
|B| (γ)
R_E
α
ψ
180
120
60
0
360
240
120
0
450
400
350
300
250
200
150
100
50
5
6
7
8
9
10
11
12
13

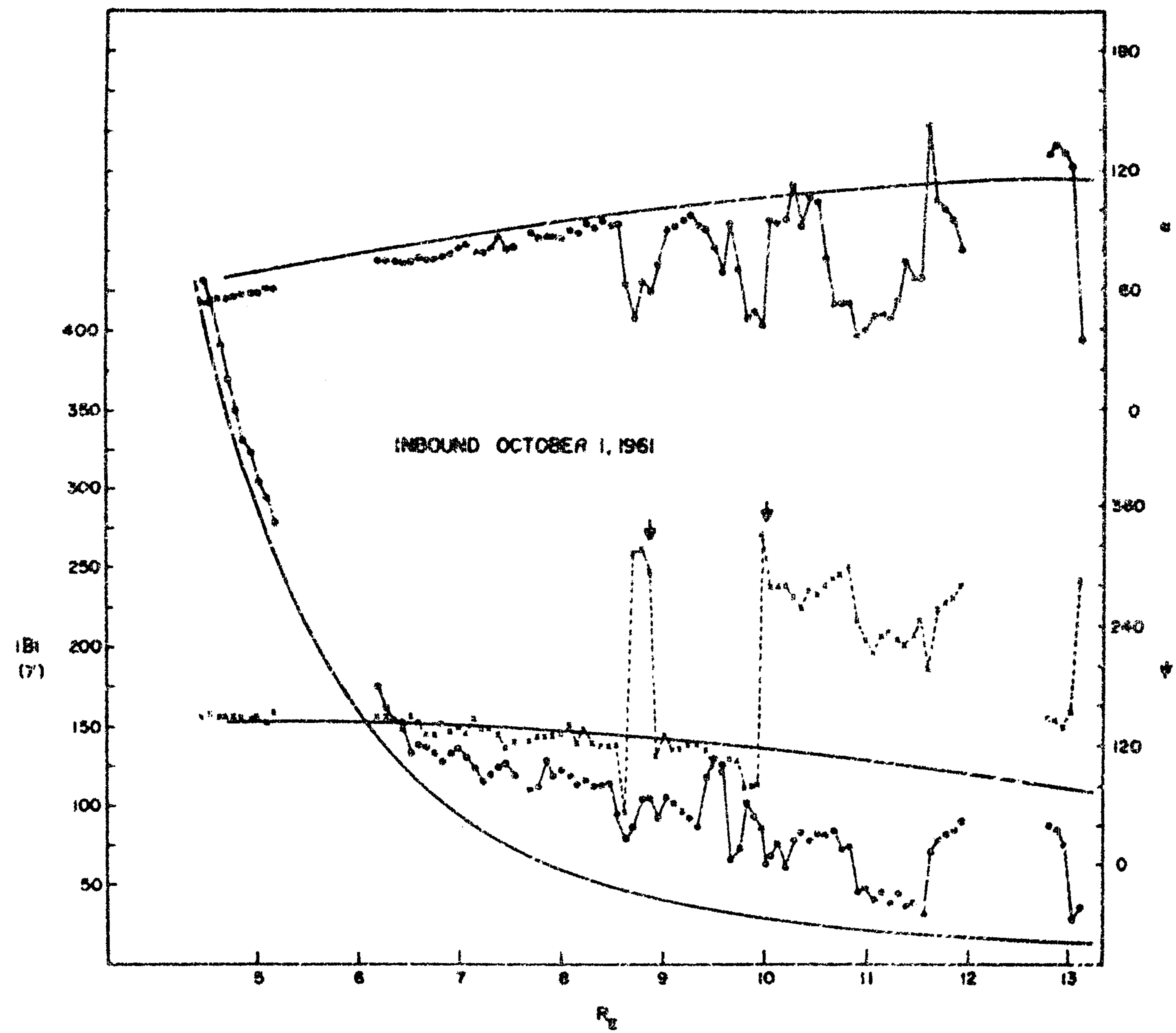

INBOUND OCTOBER 1, 1961
|B|
(γ)
400
350
300
250
200
150
100
50
5
6
7
8
9
10
11
12
13
R_E
180
120
60
0
360
240
120
0

FIG 11

FIG. 12